Perturbation Viscometer to Measure the Viscosity Gradients of Gas Mixtures

P. A. Russell, B. A. Buffham, and G. Mason
Dept. of Chemical Engineering, Loughborough University, Loughborough, Leicestershire LE11 3TU, U.K.

M. J. Heslop
Dept. of Chemical and Process Engineering, James Weir Building, University of Strathclyde, Glasgow, G1 1XJ, U.K.

Perturbation viscometry measures the logarithmic viscosity gradient of the viscosity–composition curve for gas mixtures. The flow and composition of a gas mixture flowing through a capillary are perturbed by adding a small flow of gas, normally one of the pure components of the gas mixture. Two pressure changes are seen at the capillary, the first due to the change in flow rate and the second, a short time later, due to the change in viscosity. The logarithmic viscosity gradient can be calculated from the ratio of these two pressure changes. Integration of logarithmic viscosity gradients measured over the full composition range gives the mixture viscosity relative to the viscosity of one of the pure components of the gas mixture. This method is attractive because, for measurements of equal precision, integration of the gradients is potentially an order of magnitude more precise than conventional methods that measure viscosities directly. It can also work at high and low temperatures and perhaps high pressures. The potential of this technique was previously demonstrated with a rudimentary apparatus, but its advantages and potential flaws need to be more closely examined. Here a fully thermostatted apparatus is detailed, including all modifications incorporated from experience operating the original apparatus. Experimental data for the helium–nitrogen mixture at 360°C, the practical upper operating limit of the apparatus, are presented. Integral consistency checks performed on the measured data show that high-quality data produced compare well (less than 1% deviation) with the best literature data available.

Introduction

The viscosities of gas mixtures are conventionally measured by making up a mixture at a particular composition and then measuring its viscosity using any one of the direct methods. The more popular methods currently used are capillary and oscillating-body viscometry (see Toloukian, 1975). Both of these methods are time-consuming, require precise measurement of the dimensions of the apparatus, and are difficult to apply to elevated temperatures.

Perturbation viscometry works differently. It was born out of an accidental discovery of a measurable viscosity effect produced from experiments made to measure gas adsorption isotherms for binary gas mixtures. This method measures a gradient of the viscosity–composition function. If viscosity gradients are known across the composition range, then integration of these gradients gives viscosities across the composition range relative to one of the pure components. One attraction of this method, apart from its simplicity, is that for measurements of equal precision, measurement of the differential followed by integration will be more accurate than the direct measurement of the variable itself. Another attraction is that excess data are measured that allow internal consistency checks to be made. This is not normally the case for competing methods.

Correspondence concerning this article should be addressed to P. A. Russell.

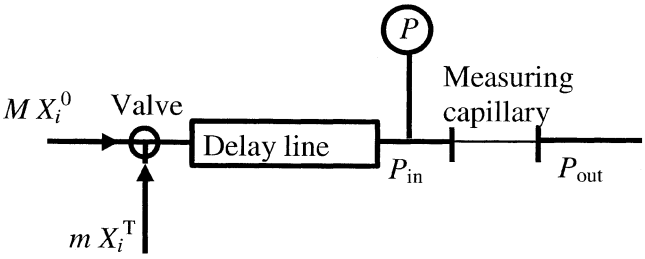

Figure 1. Basic apparatus.

In normal operation a (main) flow of gas, M, of known composition, X_i^0, flows through the valve, then a delay line (low resistance empty tube), and finally the measuring capillary tube. In an experiment, a small perturbation flow, m, composition, X_i^T is added to the main flow and the responses at the pressure gauge (one for flow-rate change, one for viscosity change) are measured. Further measurements are made when the perturbation flow is removed.

The apparatus described here is a comprehensive development of a capillary viscometer used to measure the logarithmic viscosity gradient of the viscosity–composition curve for a binary mixture (see Heslop et al., 1996, 1998 and Mason et al., 1998). The basic apparatus is shown in Figure 1. Perturbation viscometry involves changing the flow *and* composition of the main flow of gas mixture passing through a capillary tube by adding a small stream of perturbation gas (usually one of the pure components of the mixture) and monitoring the pressure changes observed at the upstream end of the capillary tube. The capillary therefore has a dual purpose: to act first as a laminar flow meter and then as a viscometer. A typical pressure record is shown in Figure 2.

Examination of the pressure record in Figure 2 shows five pressures and four pressure steps. When the perturbation flow is added, the increase in flow causes an almost instantaneous rise in pressure from P_0 to P_1. Later, when the composition front has moved through the delay line and reaches the capillary, a second pressure change from P_1 to P_2, occurs due to the change in viscosity of the mixture. When the perturbation flow is stopped, there is a pressure change P_2 to P_3 because the flow decreases, and from P_3 to P_4 when the subsequent viscosity change is detected. Note that due to the dispersion in the delay line, the viscosity pressure steps are not as sharp as those produced by the changes in flow rate. The pressure changes measured by removing the perturbation flow give a check on the data. For addition and removal of the perturbation flows we can combine the pressure steps to give two pressure ratios

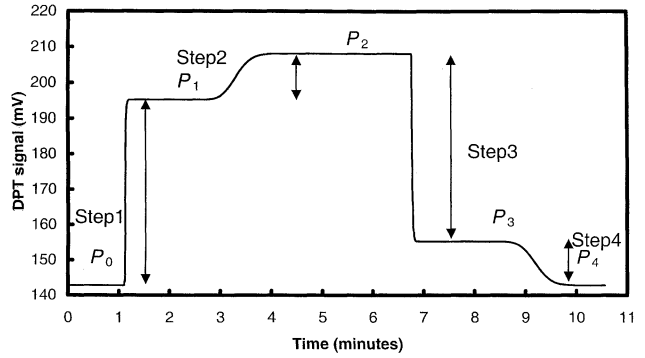

Figure 2. Pressure record for an experimental run at 360°C, where a perturbation flow of helium was added to, then removed from, a 50% nitrogen : 50% helium mixture main gas flow.

The pressure changes are: Step 1 (P_0 to P_1) due to increase in flow when perturbation is added; Step 2 (P_1 to P_2) increase in viscosity due to an increase in helium mole fraction; Step 3 (P_2 to P_3) decrease in flow when perturbation is removed; Step 4 (P_3 to P_4) decrease in viscosity due to decrease in helium mole fraction.

$$R_{\text{add}} = \frac{P_2 - P_1}{P_1 - P_0} \tag{1}$$

$$R_{\text{rem}} = \frac{P_4 - P_3}{P_3 - P_2} \tag{2}$$

For infinitesimal perturbation flows the ratios, R_{add} and R_{rem}, are both equal and proportional to $d \ln \mu / dX_i$ the logarithmic viscosity gradient (see Mason et al., 1998)

$$\frac{d \ln \mu}{dX_i} = \frac{1}{\left(X_i^T - X_i^0\right)} R_{\text{add}} = \frac{1}{\left(X_i^T - X_i^0\right)} R_{\text{rem}} \tag{3}$$

Here X_i^T is the composition of the perturbation flow, and X_i^0 is the composition of the main flow.

Mason et al. (1998) reported experiments for the addition of perturbation flows to argon–nitrogen mixtures. They found that for perturbation flows to be considered *infinitesimal,* they must be less than 0.1% of the main flow used. Perturbations of this size were found to be too small for the pressure changes to be measured accurately.

For small finite perturbation flows Mason et al. (2000) found small systematic differences between the experimental results for the added and removed perturbation flows. The systematic differences were incorporated into the theoretical treatment to produce Eqs. 4 and 5, which model the experimental results

$$\frac{\Delta \ln \mu}{\Delta X_i} = \frac{R_{\text{add}}}{\left(X_i^T - X_i^0\right)} \left[1 - \frac{m R_{\text{add}}}{2(M+m)}\right] \tag{4}$$

$$\frac{\Delta \ln \mu}{\Delta X_i} = \frac{R_{\text{rem}}}{\left(X_i^T - X_i^0\right)} \left(1 + \frac{m}{M}\right) \left[1 + \frac{m R_{\text{rem}}}{2(M-m)} \frac{M - 2m R_{\text{rem}}}{M - m R_{\text{rem}}}\right] \tag{5}$$

Each individual pressure change recorded depends on the composition of the gas in the measuring capillary when the pressure change takes place. For the flow-rate change (P_0 to P_1) observed when the perturbation is added, the gas composition inside the capillary is X_i^0. For the flow-rate change (P_2 to P_3) when the perturbation flow is removed, the gas composition inside the capillary is $X_i^0 + \Delta X_i$. The pressure steps (P_0 to P_1) and (P_2 to P_3) are, thus, *different* even though the flow-rate changes are identical. This observed difference in the flow-rate pressure steps accounts for the difference between R_{add} and R_{rem}.

This method requires only the flow rates and compositions of the gas streams to be known. Measurements at elevated temperatures are potentially simple, because *only* the measuring capillaries need to be raised to the temperature of interest.

In this article we report the design and development of a thermostatted apparatus capable of producing precise results at a range of temperatures. As a test of the method, the thermostatted apparatus was used to measure logarithmic viscosity gradients for helium–nitrogen mixtures at 360°C. This is an interesting system with a wide range of viscosity gradients over the composition range. The results obtained show that the apparatus performance is good even at elevated temperatures.

Experimental Apparatus

The experimental apparatus is based upon the preliminary design reported by Mason et al. (1998). A detailed flow sheet of the new apparatus is shown in Figure 3. To increase the sensitivity and to minimize the effects of fluctuations in the flow rate and pressure, a two-sided arrangement is used in which a differential pressure transducer measures the pressure difference between the measurement gas flow and a reference gas flow.

Flow setting block

The gas mixture enters the apparatus and is split into two streams of equal flow rate. Because a differential measurement is being made, it is crucial that both flows remain matched during the experiment. The flow-setting block is designed to produce very stable matched flows. The block has sufficient thermal mass and conducts heat well enough to maintain all components of the block at the same temperature. A single stream of gas mixture at fixed pressure is supplied to the block, which splits the gas flow internally into two equal gas flows by using a Porter high-resolution nonrising-stem needle valve followed by a Porter laminar flow element in each path. The laminar flow elements provide almost matched flow rates. The fine-control valves are used as trimmers. Downstream connections from the block are made to the rest of the apparatus by zero dead-volume connections machined into the block. It is important to minimize dead-

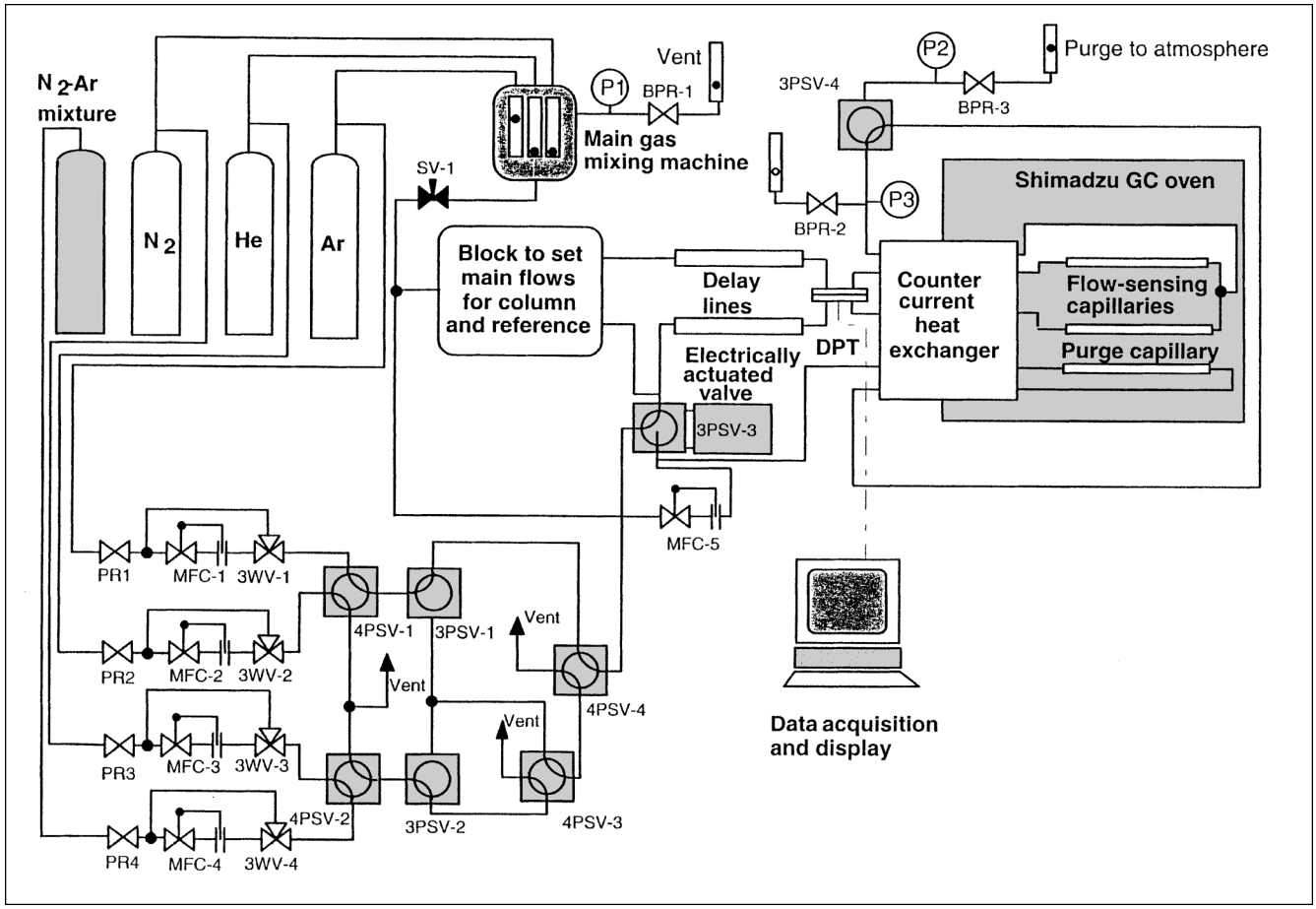

Figure 3. Flow diagram of new experimental apparatus.

BPR-1, BPR-2, and BPR-3, modified back-pressure regulators based on Porter Instruments 9000; DPT, Modified for flowthrough operation, Furness Controls FCO 40 differential pressure transducer; MFC-1, MFC-2, MFC-3, MFC-4, and MFC-5. Porter Instruments VCD 1000 flow controllers PR1, PR2, PR3, and PR4, modified Porter Instruments 8286 pressure regulators; 3PSV-1, 3PSV-2, 3PSV-3, and 3PSV-4, Valco UWE three-port switching valves; 4PSV-1, 4PSV-2, 4PSV-3, and 4PSV-4, Valco UWE three port switching valves; 3WV-1, 3WV-2, 3WV-3, and 3WV-4, SSI 02–0182.

volume if the composition is to be changed quickly. The pressure drop across the block is about 1 bar, and this delivers a flow of about 25 mL/min through each side of the apparatus.

Perturbation switching valve

The next element downstream on the measurement side of the apparatus is the perturbation switching valve, 3PSV-2. The design of this switching valve is important to the overall operation of the apparatus, particularly when precision measurements are being made. It is the only difference between the measurement side and reference side of the apparatus, and, therefore, has the possibility of introducing systematic errors.

The original prototype used a 1/16-in. Valco, three-port, two-position valve driven by a VICI ETMA microelectric two-position actuator to produce a repeatable switching action. Two adapters (Addison et al., 1994) were used to convert the valve ports to flowthrough operation. Flowthrough operation is essential because interruption of the main flow when switching the valve causes large pressure spikes. The original design had several weaknesses. First, the bore of the switching valve was small, which introduced a significant pressure drop to the measurement side and changed its dynamic response. The adapters introduced further pressure drops to the measurement side of the apparatus, which were matched by adding extra lengths of 1/16-in. tube to the reference side. These geometrical differences between the two sides further altered the dynamic response when the perturbation was switched in and out. Finally, the mechanical design of the adapters was structurally weak.

The switching valve assembly, 3PSV-2, was redesigned to overcome these shortcomings. The VICI ETMA actuator is retained, but a 1/8-in. Valco, three-port, two-position valve is used instead of the 1/16-in. valve. It has a much lower pressure drop, its bore being 1/16 in., the same as the standard tube used throughout the rest of the apparatus. The volume added to the upstream side when the valve is switched is now greater, but this is much less significant to the dynamic behavior than the reduction in pressure drop. Perhaps the most significant change is to the valve body. This has been modified to achieve flow through operation by machining two additional ports into the valve at 90° to the two gas supply ports. These have been joined to the bases of the original ports by 1/16-in.-diameter drillings. The new ports have been tapped to take Swagelok 1/8- to 1/16-in. stainless steel reducing unions that have been bored through to a diameter of 1/16 in. and sealed with rubber O rings. The bore of the valve assembly carrying the main flow is never less than 1/16 in., and is matched by an extra length of 1/16 in. bore tubing in the reference side of the apparatus. Both streams now have very similar dynamic behavior.

Pipework

Most of the pipework has been standardized on tube of 1/8-in. OD, 1/16-in. bore. These dimensions were found to give the best compromise between minimizing the pressure drop and causing inconvenient delay. Nylon tube (1/8-in. OD) is used for all low-temperature pipework and stainless steel for the heated regions of the apparatus. Exceptions to this are the delay lines and the measuring capillaries (described later). The delay lines are two 1.5-m-long, 1/4-in. OD tubes. They delay the arrival of the composition change at the measuring capillary tube, and, thus, separate the effects of flow rate and viscosity changes.

When helium was used in the original apparatus, gas density gradients in vertical pipe runs produced pressure fluctuations (the manometer effect). To prevent this, in the current apparatus all pipework is aligned to within 50 mm of a horizontal datum.

Flowthrough pressure transducer design

The Furness Instruments differential pressure transducer (DPT) is the next major item downstream and is the heart of this apparatus. It is a diaphragm type using a capacitance sensor and has a pressure range of $\pm$10-mm water giving a $\pm$1-V output. The standard design, while accurate, has a serious defect for this application: gas of the new composition does not sweep through the transducer itself when the perturbation flow is added. Gas of the original composition trapped in the transducer and impulse lines slowly diffuses into the main flow and causes a slight systematic drift in the plateaus in the DPT signal.

We commissioned a special transducer from Furness Instruments with extra ports to let the main gas flow pass through its measurement chambers. This required an extra pressure tapping to be added to each side of the transducer. The main flow now enters each side of the transducer through the original ports and leaves via the new ports. The gas composition inside the transducer is now always the same as the main gas flow. This has eliminated the systematic drift.

The gas flow through the new transducer made it inherently more noisy than its predecessor. Various methods have been employed to reduce this undesirable noise. Increasing the bore of the transducer tappings to 1/16 in., which reduces the pressure drop through the transducer, reduces the flow-induced noise. The electronic noise in the transducer was reduced by 50% by changing its TL062CP chip amplifier for a TL072CP amplifier. Furthermore, a simple damping circuit of a 300-Ω resistance and 4.7-μF capacitor was used to remove all electrical noise above 25 Hz. A remote 16-bit A/D converter (Adept Scientific data shuttle) is used to digitize the transducer analog signal at the transducer and eliminate noise produced during data transfer. Data acquisition is controlled by Workbench PC software, run using the low-noise 50-Hz operating mode. Data are logged at 25 Hz, at which frequency experiments have shown the lowest noise. The end result of these noise-reduction measures for the three pressure plateaus corresponding to the addition of the perturbation gas is illustrated in Figure 4. These short-term noise levels are similar to those obtained from the original diffusion transducer, but the high-frequency noise has been removed to reveal the true signal variation.

Heat exchanger

A countercurrent heat exchanger is located after the pressure transducer to preheat the gas to the operating temperature of the capillaries. It is crucial that gas temperatures in the heat exchanger remain steady, otherwise expansion and

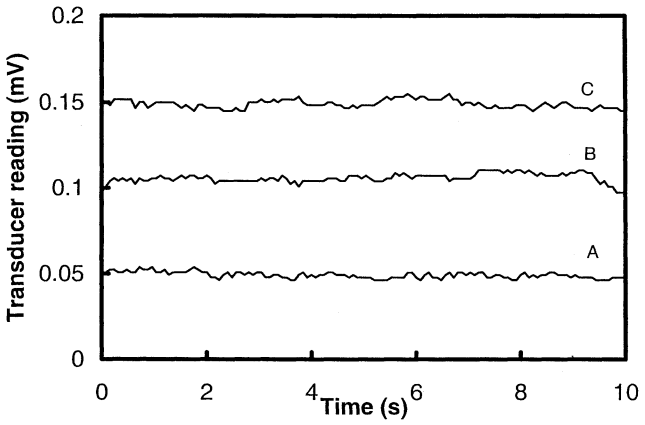

Figure 4. Character of short-term noise taken from the experimental run using a main flow composition 50:50 of helium–nitrogen and a helium perturbation flow.

The three traces *A*, *B* and *C* shown are 10-s segments taken, respectively, from each of the three pressure plateaus P_0, P_1, and P_2 for addition of the perturbation flow (see Figure 2). The noise bandwidth for these segments is 0.02 mV, which is marginally greater than the minimum resolution of the data-acquisition hardware. *B* and *C* are marginally more noisy, because the flow now contains the additional flow of the perturbation gas.

contraction of the gas produces flow-rate changes that appear as noise on the pressure record (see Meacham et al., 1993). The heat exchanger is made in two parts. The first stage of the heat exchanger is made from five 1/8-in. stainless steel tubes welded together. Two of these tubes take the measurement and reference gas streams to the capillary tubes inside the oven. The ends of the capillaries are connected together inside the oven, and the mixed gas of the measurement and reference flows leaves the oven through a third tube. The two remaining tubes carry a purge stream into and out of a third capillary in the oven (see below). The tube bundle is enclosed for half its length by the oven and encased in brass sheaths to increase thermal stability. The second part of the heat exchanger is a brass manifold block. All connections to and from the capillaries are made through this block.

The measuring capillaries assembly

The final major elements are the downstream measuring capillaries. The downstream measuring capillaries generate the pressure difference sensed by the pressure transducer. These are two 0.5-m-long stainless steel tubes, 1/16-in. OD, 0.043 in. bore. The pressure drop through each is about 0.13 mmHg when the gas flow is 25 mL/min at 25°C.

A brass former is used to support the capillaries and provide thermal stability. Two helical grooves, starting 180° degrees apart, are screw-cut clockwise along the surface of the cylindrical former to a depth of 3/16 in. A second pair of helical grooves 1/8-in. deep, each starting 90° from the first pair, are cut anticlockwise into the block surface. Each capillary tube is wound along the block in the 3/16-in. groove and then back in the adjacent 1/8-in. groove. Thus, all connections to the capillaries are made at the same end of the former.The tubes fit tightly into the grooves, ensuring good thermal contact with the block. All connections from the capillaries are made to the manifold. The entire block-and-tube assembly is wrapped in aluminium foil to minimize heat transfer by radiation. The temperature is measured by a K-type steel-sheathed thermocouple with its junction in the center of the brass former. The assembly is mounted inside a Shimadzu GC-8A gas chromatograph oven that controls the temperature to better than ± 0.1°C. The thermal mass of the brass support block damps out temperature fluctuations and maintains the difference in the temperature between the capillaries to less than 1×10^{-5}°C (measured by transducer "noise" and drift). The brass block is supported on a spring-mounted platform inside the oven to isolate the capillaries from vibration. The assembled heated portion of the apparatus is shown in Figure 5. (The aluminum foil has been removed to expose the capillaries wound onto the brass former.)

Purge stream

When adding or removing the perturbation flow, sharp spikes in pressure occur unless the pressures on both sides of the addition valve are exactly equal. This is because the valve rotor carries a small volume of gas. In order to keep the pressure in the perturbation stream exactly the same as the main flow, even when the perturbation stream is not being added, a third or purge stream is required. The perturbation flow joins this stream when it is not added to the main flow. The geometry of the pipework for the purge flow must be similar to that for the main flow and connected to the same outlet back-pressure regulator to give matched pressure drops. Temperature control of this stream is not critical, but the pressure is more easily kept constant if the stream flows through a third matched capillary tube wound directly onto the outside of the capillary support block. The pressure drop down it then varies with temperature in much the same way as the pressure drop in the reference and measuring sides for the system.

Perturbation flow supply system

The perturbation flow system is connected to the main flow at valve 3PSV-2. The perturbation flow rate is about 0.5 mL/min so that it takes a long time to flush a change in composition through the system. Consequently, the pipework is modified to allow the controller to be bypassed by a higher flow of gas. The layout is shown in Figure 3. A Porter mass flow controller sets the perturbation flow downstream of a pressure regulator. The bypass around the mass-flow controller permits the perturbation system to be purged with the new perturbation gas when the perturbation gas type is changed. A sequence of three- and four-way valves permits any of four perturbation gases to be used individually and higher flows to be generated without affecting the flows set by the mass-flow controllers. The system also allows the possibility of making up mixtures of any two perturbation gases by blending two of the pure perturbation gases together. This is particularly useful when using a pure component as the main gas flow.

Experimental Method

An experiment lasts about 10 minutes and involves recording the pressure changes for first adding the perturbation flow

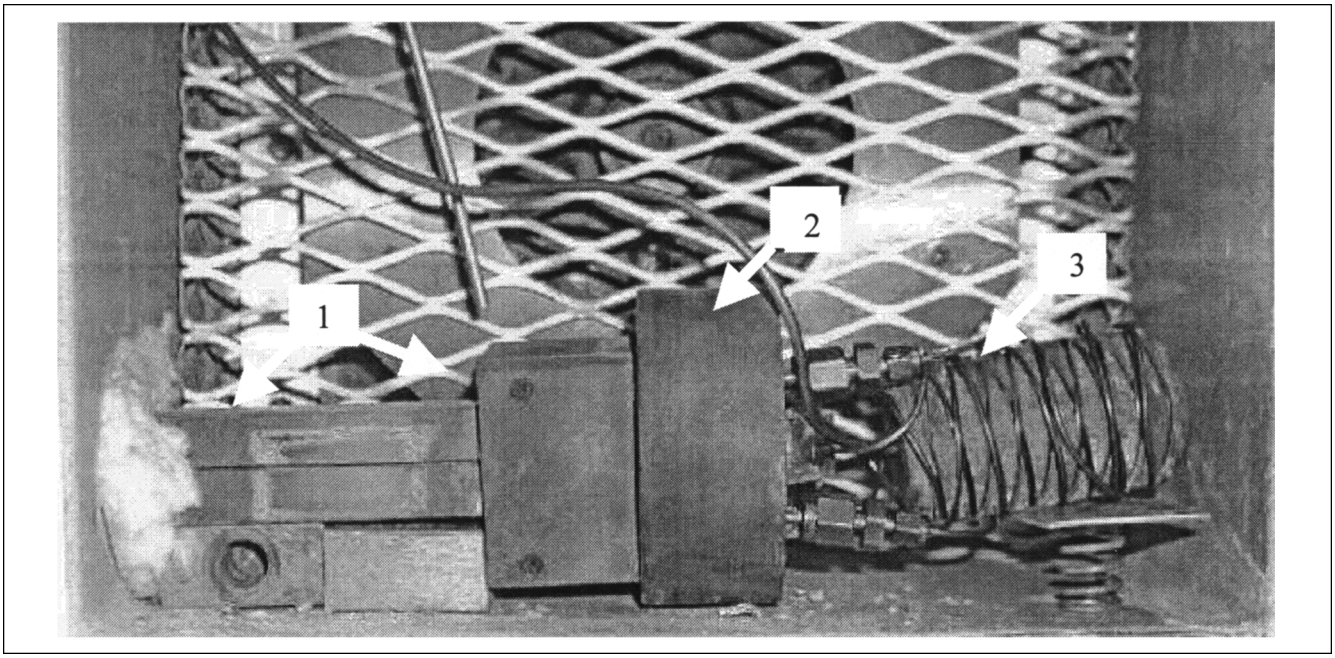

Figure 5. Heated section of the apparatus is shown assembled and mounted inside the Shimadzu GC oven.

(1) Heat shields on the tube bundle heat exchanger, (2) manifold block, (3) brass spiral-cut former supporting the measuring capillaries.

and then removing it in a single data file, as indicated in Figure 2. This method was adopted to enable the "remove" perturbation pressure-change sequence to be used as a check on the "addition" perturbation data for constant conditions.

During an experiment some drift in the base line is sometimes observed. It was usually less than 0.1 mV over the total run time. The data records are processed using a separate computer program that samples 400 data points in two parts of each pressure plateau and calculates the average of the sample group for each plateau. The program also calculates the linear gradient of the base line as it drifts over the total run and corrects the measured pressure changes for this small but not completely insignificant effect. The drift in the base line is, in part, dependent on the size of the perturbation flow and increases significantly if very large perturbations are used. This may be a consequence of the dynamic response time of the downstream back pressure regulator.

Experimental Results

Viscosity gradients were measured for the helium–nitrogen mixture at 360°C. This temperature was chosen as the maximum stable temperature achievable with the Shimadzu GC-8A oven. All measurements were made using gases of 99.99% purity supplied by the British Oxygen Company. Measurements were made using each of the two pure gases as perturbation gas, for main flow compositions at nominal 0.1-mole-fraction intervals across the composition range. The main gas flow mixtures were prepared using a gas blender of our own design. The results obtained are recorded in Table 1. Some experiments were repeated to give a measure of their reproducibility. The difference is about 0.0005 in the logarithmic viscosity gradient. This is comparable to the noise measured in the pressure plateaus.

The data can be checked for consistency by examining the differences in the logarithmic viscosity gradients, $(\Delta \ln \mu / \Delta X_i)_{\text{add}} - (\Delta \ln \mu / \Delta X_i)_{\text{rem}}$, obtained when adding and removing each perturbation gas for each experimental run. These differences are plotted against the helium mole fraction in Figure 6. At each composition the main flow composition was kept constant, and pure nitrogen and helium were used in turn as the perturbation gas.

Ideally for each main flow composition the logarithmic viscosity gradients should be the same for adding and removing the perturbation flow. For the composition range 0.2- to 0.8-mole-fraction helium, the data are randomly scattered, but exhibit a slight positive bias and lie within an error band of ± 0.002. The bias observed is the result of density differences between the measurement and reference sides of the apparatus. When the perturbation flow is added, the gas mixture density (mass) is changed. If the flow paths in the apparatus are not in the same horizontal plane for both sides of the apparatus, small pressure changes (buoyancy) will be seen as the composition front moves through the apparatus. The apparatus is particularly sensitive to differences in the alignment between the delay lines and the pressure transducer. This problem had been identified and addressed when the apparatus was redesigned. The redesign eliminated most of the pressure fluctuations due to density changes. However, the large density difference for the components of this mixture produced a residual effect that is just detectable as the positive bias seen for the results of this test.

For the nitrogen perturbation at concentrations less than 0.2-mole-fraction helium and the helium perturbation at concentrations greater than 0.8-mole-fraction helium, the error increases with concentration. If the gradients for these individual data points are compared with the gradients for the opposite perturbation gas at similar compositions, all of the

Table 1. Logarithmic Viscosity Gradients Measured for Nitrogen-Helium Mixtures at 360 °C

Mole Fraction Helium, X_{He}		Log. Vis. Grad., $(d \ln \mu)/dX_{He}$	
		Exp. with Perburbation	
Main Flow	Perturb. Gas	Added	Removed
0.0958	0	0.1068	0.1020
0.0989		0.1077	0.1044
0.1920		0.1098	0.1086
0.3038		0.1136	0.1116
0.3038		0.1139	0.1119
0.3982		0.1195	0.1174
0.3982		0.1192	0.1179
0.5022		0.1187	0.1183
0.6011		0.1159	0.1152
0.6922		0.1049	0.1041
0.7812		0.0826	0.0835
0.8721		0.0349	0.0342
0.9839		−0.0967	−0.0966
0.9839		−0.0970	−0.0962
0.0207	1	0.0978	0.0976
0.1161		0.1041	0.1036
0.2128		0.1101	0.1099
0.3241		0.1159	0.1154
0.4191		0.1184	0.1180
0.5225		0.1198	0.1201
0.6210		0.1155	0.1146
0.7111		0.1027	0.1014
0.8366		0.0599	0.0621
0.8366		0.0611	0.0608
0.8904		0.0205	0.0238
0.8904		0.0202	0.0238
0.8917		0.0032	0.0026
0.9376		−0.0281	−0.0216

error appears to be when helium is added to helium-rich mixtures and nitrogen to nitrogen-rich mixtures. This may be expected because the composition changes, and, hence, the size of the viscosity steps for these perturbations, are very small.

For a single main flow composition, the logarithmic viscosity gradients for each perturbation gas cannot be compared directly. Each perturbation gas moves the mean composition in a *different* direction by a *different* amount. The measured

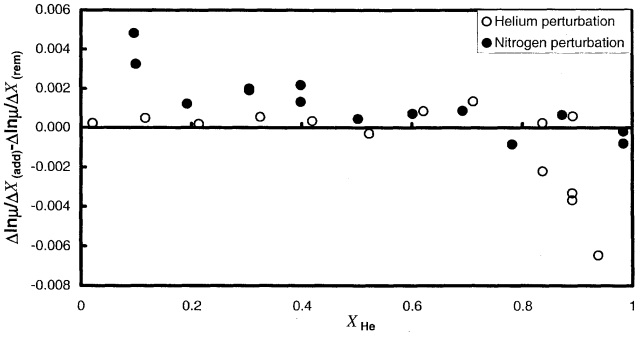

Figure 6. Errors in the data set are illustrated for the helium–nitrogen mixture using a graph of the difference $(\Delta \ln \mu/\Delta X)_{add}-(\Delta \ln \mu/\Delta X)_{rem}$ vs. helium mole fraction at 360°C.

The error is seen to increase for measurements made at the ends of the composition range where the composition change $(X_i^T - X_i^0)$ is small.

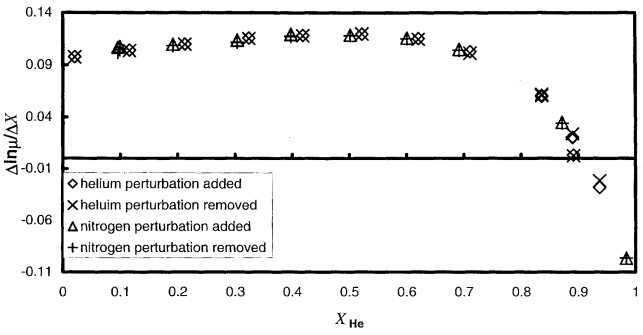

Figure 7. Second consistency test of the data is applied by plotting of $(\Delta \ln \mu/\Delta X)$ vs. helium–mole fraction for all experimental measurements made on the helium–nitrogen mixture at 360°C.

All data points lie on a common curve except for the pair of data points measured where the curve cuts the X-axis and the measured gradient approaches zero. This data point is subject to the largest errors, because the measured pressure change for the viscosity step is very small.

gradient is taken to occur at the center of the composition change produced by adding each perturbation gas. Therefore, if each of the perturbation gases is added to the same main flow, the gradients measured will have different values because they refer to slightly different compositions. However, all the values should lie on the same composition −viscosity gradient curve. This is the second check that can be applied to the data set (see Figure 7). Most of the points do lie on a continuous smooth curve. As expected there are quite large errors in the points where helium is added to helium-rich mixtures and vice versa with nitrogen.

These data can also be tested by comparing them with data from other sources. No other method exists for measuring logarithmic viscosity gradients, and no actual experimental absolute viscosity data exist for this mixture at 360°C. Kestin et al. (1972) have measured absolute viscosities at temperatures up to 700°C. They fitted all of their data using the Chapman-Enskog theory to relate the mixture viscosity to temperature and composition for temperatures up to 700°C. Their Chapman-Enskog fit has been used to calculate a smoothed data set of absolute viscosities at 360°C that can be compared with our new results.

For comparison it is necessary to convert our gradient data to relative viscosities by integration of the logarithmic viscosity gradient data across the composition range. Because of the complex behavior of the viscosity of the helium−nitrogen mixture, we used a sixth-order polynomial to achieve a satisfactory fit of the data. Integration by this fitted polynomial was used to calculate the viscosity of the mixture relative to the viscosity of helium.

The mixture viscosities relative to the viscosity of helium at 360°C are plotted for both data sets in Figure 8. The stated accuracy of the Kestin et al. (1972) smoothed data for the absolute viscosities is better than 0.6%. For main flow compositions in the range 0 to 0.7 helium mole fraction, our new data agree to better than 0.1% with the smoothed data. For main flow compositions above 0.7 helium mole fraction, the agreement is not quite as good at 0.2% agreement with the

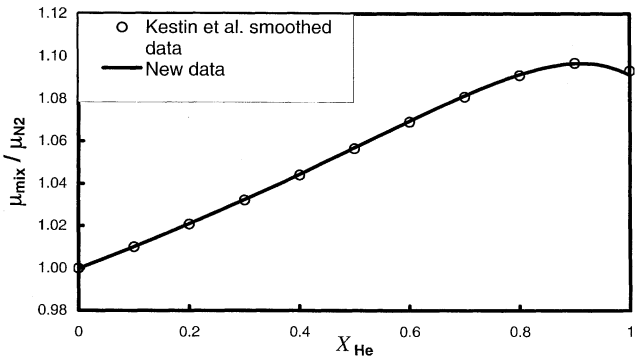

Figure 8. Relative viscosities for the nitrogen–helium gas mixture at 360°C.

The smooth curve represents the integrated polynomial obtained from the numerical fit of the viscosity gradient data measured using the new apparatus. It shows very good agreement with the smoothed experimental values measured by Kestin et al. (1972), shown as discrete points.

smoothed data. In any event the two data sets agree to better than the stated accuracy of the smoothed data over the whole composition range.

Error Analysis

The consistency checks performed so far give a qualitative indication that the data produced is consistent. It is possible to go much further to obtain a quantitative feel for the uncertainties in the measured parameters. We are lucky in that we know that the logarithmic viscosity gradient (G) is a function of the pressure ratio R and the composition change $(X_i^T - X_i^0)^{-1}$

$$\frac{\Delta \ln \mu}{\Delta X} = G = R\left(X_i^T - X_i^0\right)^{-1} \tag{6}$$

This expression can be expanded using the propagation-of-errors theory (see Bevington and Robinson, 1994) to give an expression to account for the uncertainties in each measured variable

$$\partial G = \frac{\partial R}{\left(X_i^T - X_i^0\right)} + \frac{R\partial X_i^T}{\left(X_i^T - X_i^0\right)^2} + \frac{R\partial X_i^0}{\left(X_i^T - X_i^0\right)^2} \tag{7}$$

Division through by G will give the fractional errors

$$\frac{\partial G}{G} = \frac{\partial R}{R} + \frac{\partial X_i^T}{\left(X_i^T - X_i^0\right)} + \frac{\partial X_i^0}{\left(X_i^T - X_i^0\right)} \tag{8}$$

The fractional error in the measured pressure ratios $\partial R/R$ can be estimated from the difference between the gradients measured when a pure perturbation gas is added to and removed from the main flow of a single component gas. Under these special conditions the error terms ∂X_i^T and ∂X_i^0 must tend toward zero and can be ignored because both the main and perturbation streams are pure gases. For this mixture the error term $\partial R/R$ is estimated to be approximately 0.84%.

The composition error in the ∂X_i^T and ∂X_i^0 terms can be calculated by two different routes. Route 1 uses the difference between the gradients measured by adding and removing the perturbation flow to a mixture, as with consistency test 1. For this method the ∂X_i^T term is zero because the same perturbation is used for both gradient measurements. The equation therefore becomes

$$\frac{\partial X_i^0}{\left(X_i^T - X_i^0\right)} = \frac{G_{\text{add}} - G_{\text{rem}}}{G_{\text{add}}} - \frac{\partial R}{R} \tag{9}$$

Route 2 calculates the fractional error in the viscosity gradient using the difference between the gradient measured when adding the perturbation and the value calculated from the curve fitted through all the measured gradients. This curve was obtained when integrating the data for consistency test 3 and will be assumed to represent the true gradient–composition relationship. Under this condition, for a given perturbation gas, ∂X_i^T will have a constant size dependent on the level of impurity in the pure gas. The equation therefore becomes

$$\frac{\partial X_i^0}{\left(X_i^T - X_i^0\right)} = \frac{G_{\text{add}} - G_{\text{calc}}}{G_{\text{add}}} - \frac{\partial R}{R} + \frac{\partial X_i^T}{\left(X_i^T - X_i^0\right)} \tag{10}$$

A least-square minimization can now be performed on the difference between the composition errors obtained from each of the two routes using Eq. 11 for all data points measured using the same perturbation gas

$$\Sigma_i \left[\left(\frac{G_{\text{add}} - G_{\text{rem}}}{G_{\text{add}}} - \frac{\partial R}{R} \right) - \left(\frac{G_{\text{add}} - G_{\text{calc}}}{G_{\text{add}}} - \frac{\partial R}{R} + \frac{\partial X_i^T}{\left(X_i^T - X_i^0\right)} \right) \right]^2 \tag{11}$$

The value of ∂X_i^T is the only parameter varied in the minimization routine, and its final value is the best estimate of the error in this parameter. The error in the main flow composition ∂X_i^0 is the error band for all data points calculated using the best estimate of ∂X_i^T. For this mixture the error ∂X_{i}^0 was found to be $\pm 2\%$. The errors for the perturbation composition ∂X_i^T were found to be -0.34% for the helium perturbation and -0.86% for the nitrogen perturbation.

From the estimates of ∂R, ∂X_i^0, and ∂X_i^T it is obvious that the main source of the error in the viscosity gradient comes from the composition of the main flow. The main flow mixtures are prepared from two or more flows of pure gas, each of which is measured independently with a soap-bubble flowmeter. The measurement relies on the skill of the operator timing a soap-bubble rise between two fixed points with a stopwatch. Thus, typical errors of 0.5% are to be expected in each gas flow measured. The error in each gas flow measured will increase as the flow rate for each component diverges at the ends of the composition range and becomes more difficult to measure. Measurements can also be compromised by gas diffusing through the soap film, the vapor pressure of the film, and liquid draining down the wall of the flowmeter. Ac-

curate determination of the gas mixture composition is difficult and has been identified as the main source of error in gas viscosity measurements made by other workers (see Kestin and Leidenfrost, 1959, and Iwasaki and Kestin, 1966). Thus, cumulative errors in this composition term of 2% are not unreasonable.

Of more concern is the error observed in ∂X_i^T. These should be much smaller than those estimated because the gases were supplied as 99.99% pure. The estimates were obtained from gradient values calculated using the fitted polynomials and, therefore, depend on the ability of the polynomial to represent the viscosity–composition function. This may account for some of the discrepancy. However, it does not account for all of the error difference, especially in the value of ∂X_i^T of -0.0084 mole fraction for the nitrogen perturbation. In an attempt to resolve this, the nitrogen supplied was examined using a mass spectrometer. The results were inconclusive, but did seem to suggest that at least 0.1% argon was present as a contaminant.

Conclusions

We have developed a new capillary viscometric technique based on making differential measurements. The technique and apparatus have been shown to work with no reduction in performance up to 360°C. By the use of internal consistency checks it has been shown that the apparatus produces viscosity-gradient data of very high quality. Integration of the experimental gradient data produces relative viscosity data that are at least as good as if not superior to existing data. The method is relatively fast, simple, and has the potential to work at much higher pressures and temperatures.

Notation

G = logarithmic viscosity gradient
m = molar flow rate of perturbation gas
M = molar flow rate of main-flow gas
P_0 = pressure at gauge before perturbation flow added
P_1 = pressure at gauge after perturbation flow added
P_2 = pressure at gauge after viscosity change has occurred
P_3 = pressure at gauge after perturbation flow removed
P_4 = pressure at gauge after viscosity change has occurred
R = ratio of viscosity pressure change to flow pressure change
T = temperature
X = mole fraction

Greek letters

μ = viscosity
Δ = a small but finite difference

Subscripts and superscripts

Ar = Argon
He = Helium
N_2 = Nitrogen
i = species i
add = adding perturbation
rem = removing perturbation
calc = value calculated from polynomial fitted through all measured gradients
0 = main flow gas
T = perturbation gas

Literature Cited

Addison, P. A., B. A. Buffham, G. Mason, and G. D. Yadav, "Gas-phase Dispersion Assessed from Tracer Hold-Up Measurements on a Packed Bed: Theory, Apparatus and Experimental Test (or How to Measure Dispersion with a Pressure Gauge)," *Chem. Eng. Sci.*, **49**, 561 (1994).

Bevington, P. R., and D. K. Robinson, *Data Reduction and Error Analysis for the Physical Sciences*, 2nd ed., McGraw-Hill, New York (1994).

Heslop, M. J., B. A Buffham, G. Mason, and N. Ireland, "New Method to Estimate Binary Gas-Mixture Viscosities," *Inst. Chem. Eng. Res. Event*, Leeds, **2**, 934 (1996).

Heslop, M. J., G. Mason, and B. A. Buffham, "A Consistency Test in the Determination of Binary Gas Mixture Viscosities," *Inst. Chem. Eng. Res. Event*, Newcastle, CD-ROM Record Nos. 13,098–13,161 (1998).

Iwasaki, H., and J. Kestin, "The Viscosity of Argon-Helium Mixtures," *Physica*, **29**, 1345 (1963).

Kestin, J., and W. Leidenfrost, "The Effect of Pressure on the Viscosity of N_2–CO_2 Mixtures," *Physica*, **25**, 525 (1959).

Kestin, J., S. T. Ro, and W. A. Wakeham, "Viscosity of the Binary Gaseous Mixture Helium–Nitrogen," *J. Chem. Phys.*, **56**, 4036 (1972).

Mason, G., B. A. Buffham, M. J. Heslop, and B. Zhang, "Capillary Viscometry by Perturbation of Flow and Composition," *Chem. Eng. Sci.*, **53**, 2665 (1998).

Mason, G., B. A. Buffham, M. J. Heslop, P. A. Russell, and B. Zhang, "Perturbation Viscometry of Gas Mixtures. Addition and Removal of Finite Perturbations," *Chem. Eng. Sci.*, **55**, 5747 (2000).

Meacham, R. I., M. J. Heslop, B. A. Buffham, and G. Mason, "Causes and Elimination of Noise in Sorption-Effect Chromatography, II: Thermal Noise," *J. Chromatog. Sci.*, **31** (1993).

Touloukian, Y. S., S. C. Saxena, and P. Hestermans, *"Viscosity" Thermophysical Properties of Matter,* The TPRC Data Series, Vol. 11, Plenum, New York (1975).

Manuscript received May 22, 2002, revision received Dec. 16, 2002, and final revision received Apr. 21, 2003.